ELSEVIER

Chemical Physics 228 (1998) 181–184

Chemical Physics

Theoretical treatment of state-selective one-electron capture by S^{3+} ions in collisions with helium

M.C. Bacchus-Montabonel

Laboratoire de Spectrométrie Ionique et Moléculaire (UMR 5579), CNRS et Université Lyon I 43, Bd du 11 Novembre 1918 69622 Villeurbanne Cedex, France

Received 17 September 1997

Abstract

Ab-initio potential energy curves and coupling matrix elements of the molecular states involved in the collision of the S^{3+} multicharged ion on helium have been determined by means of configuration interaction methods. The total and partial electron capture cross sections for the S^{3+}/He system have been determined using a semi-classical method in the 2–50 keV laboratory energy range. The results show a decrease of the cross-section on the $S^{2+}(^1D)$ level for increasing collisional energy, in good agreement with experimental data. © 1998 Elsevier Science B.V.

PACS: 34.70

1. Introduction

Charge transfer recombination of multiply charged ions in collision with atomic hydrogen and helium is an important process in astrophysical plasmas [1–3] as well as in controlled thermonuclear fusion research [4,5]. A full theoretical treatment involving an ab-initio molecular calculation of the potential energy curves and couplings followed, according to the collision energy range, by a semi-classical or a quantal collision dynamics taking account of translation effects, has been shown to provide a quantitative interpretation of theses processes [6,9]. The use of ab-initio potentials allows, in particular, to extend the approach to open-shell systems involving several outer electrons as low-charged [7], or metastable multicharged ions [9].

We have thus undertaken a complete study of the S^{3+} + He state selective electron capture reaction for which astrophysical implications are important as highlighted by McCray et al. [10] and Péquignot et al. [2]. Moreover, translational energy experiments associated with a multichannel Landau-Zener approach have been performed in the 2–9 keV energy range by Wilson et al. [11]. We report in this paper an ab-initio molecular treatment of the $S^{3+}(3s^2 3p)^2P + He(1s^2)^2S$ reaction taking into account the Σ and Π adiabatic states correlated to the entry and the most important one-electron capture channels. Regarding the collision energy range, dynamics have been performed by means of a semi-classical formalism including translation effects.

2. Molecular calculations

The adiabatic states of SHe^{3+} correlated to the ground state $S^{3+}(3s^2 3p)^2P$ entry channel and the

PII S0301-0104(97)00359-5

three main one-electron capture channels are designed below :

$$S^{3+}(3s^2 3p)^2P + He(1s^2)^1S \qquad {}^2\Sigma^+, {}^2\Pi \qquad (1)$$

$$S^{2+}(3s^2 3p^2)^1S + He^+(1s)^2S \qquad {}^2\Sigma^+ \qquad (2)$$

$$S^{2+}(3s^2 3p^2)^1D + He^+(1s)^2S \qquad {}^2\Sigma^+, {}^2\Pi, {}^2\Delta \qquad (3)$$

$$S^{2+}(3s^2 3p^2)^3P + He^+(1s)^2S \qquad {}^{2,4}\Sigma^+, {}^{2,4}\Pi \qquad (4)$$

A fourth exit channel,

$$S^{2+}(3s^2 3p^2)^3D + He^+(1s)^2S \qquad {}^{2,4}\Sigma, {}^{2,4}\Pi, {}^{2,4}\Delta$$

corresponding to a very long range avoided crossing with the entry channel has not been taken into account. As far as spin-orbit effects may be neglected in the collision energy range of interest, only spin doublet states have been considered. Moreover, the entry channels being of Σ and Π symmetry, the Δ state correlated to $S^{2+}(3s^2 3p^2)^1D + He^+$ may influence the collision by means of rotational coupling only.

The potential energy curves have been determined by means of MCSCF + CI calculations with configuration interaction (CI) based on the CIPSI algorithm [12]. Relatively compact configuration interaction spaces, about 500 determinants, have been used in the calculation with a threshold $\eta = 0.005$ for the perturbation contribution to the wavefunction. For helium, we took the (6s1p) contracted to (4s1p) basis set already used in the study of multicharged ion–helium collisions [8]. For sulfur, an optimized (13s10p2d) contracted to (6s5p2d) basis set has been constructed from the basis sets proposed by Chandler et al. [13]. Table 1 shows a quite good agreement with experiment [14] for the atomic energy levels, the discrepancies are in the range 0.016–0.082 eV.

Σ, Π and Δ potential energy curves corresponding to the ground state entry channel $\{S^{3+}(3s^2 3p)^2P + He\}$ are presented in Fig. 1. Σ curves show an avoided crossing at $R = 8.0$ au between the entry channel and the $S^{2+}(^1S) + He^+$ exit channel and another one at $R = 6.0$ au with the $S^{2+}(^1D) + He^+$ level which is also exhibited on the Π potential energy curves. A wider one is displayed at about $R = 5.5$ au involving the $S^{2+}(^3P) + He^+$ capture channel.

Table 1
Comparison with experiment [14] of asymptotic energy values for single electron capture Σ levels (in eV)

	CIPSI calculation [10]	Experiment
$S^{3+}(3s^2 3p)^2P + He$		0.0
$S^{2+}(3s^2 3p^2)^1S + He^+$	−7.0202	−7.1018
$S^{2+}(3s^2 3p^2)^1D + He^+$	−9.0827	−9.0664
$S^{2+}(3s^2 3p^2)^3P + He^+$	−10.4541	−10.3915

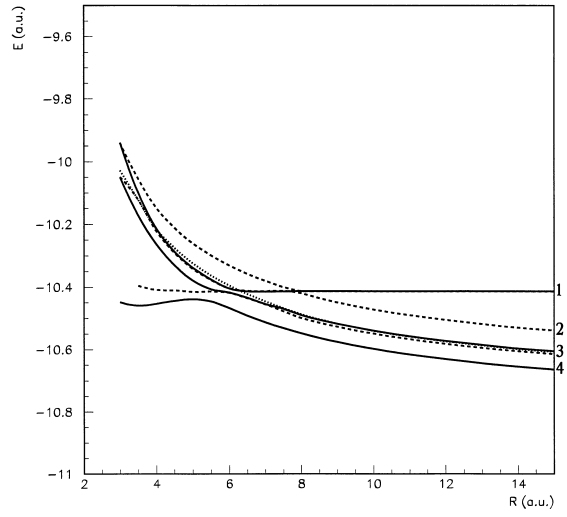

Fig. 1. Adiabatic potential energy curves for the $^2\Sigma$, $^2\Pi$ and $^2\Delta$ states of SHe^{3+}. --- $^2\Sigma$; — $^2\Pi$; · · · $^2\Delta$. 1: Σ, Π states dissociating to $\{S^{3+}(3s^2 3p)^2P + He^+(1s)\}$; 2: Σ state dissociating to $\{S^{2+}(3s^2 3p^2)^1S + He^+(1s)\}$; 3: Σ, Π Δ states dissociating to $\{S^{2+}(3s^2 3p^2)^1D + He^+(1s)\}$; 4: Σ, Π states dissociating to $\{S^{2+}(3s^2 3p^2)^3P + He^+(1s)\}$.

The radial coupling matrix elements between all pairs of states of the same symmetry have been calculated by means of the finite difference technique [15]:

$$g_{KL}(R) = \langle \Psi_K | \partial/\partial R | \Psi_L \rangle = \lim_{\Delta \to 0} \frac{1}{\Delta} \langle \Psi_K(R) | \Psi_L(R + \Delta) \rangle,$$

with the parameter $\Delta = 0.0012$ au as previously tested and using the sulfur nucleus as origin of electronic coordinates.

The radial coupling matrix elements are displayed in Fig. 2a,b. They present the same features as exhibited by the potential energy curves with a sharp peak for the crossing at $R = 6.0$ au corresponding to a transition to the $S^{2+}(^1D) + He^+$ capture channel. The rotational coupling matrix elements $\langle \Psi_K | iL_y | \Psi_L \rangle$

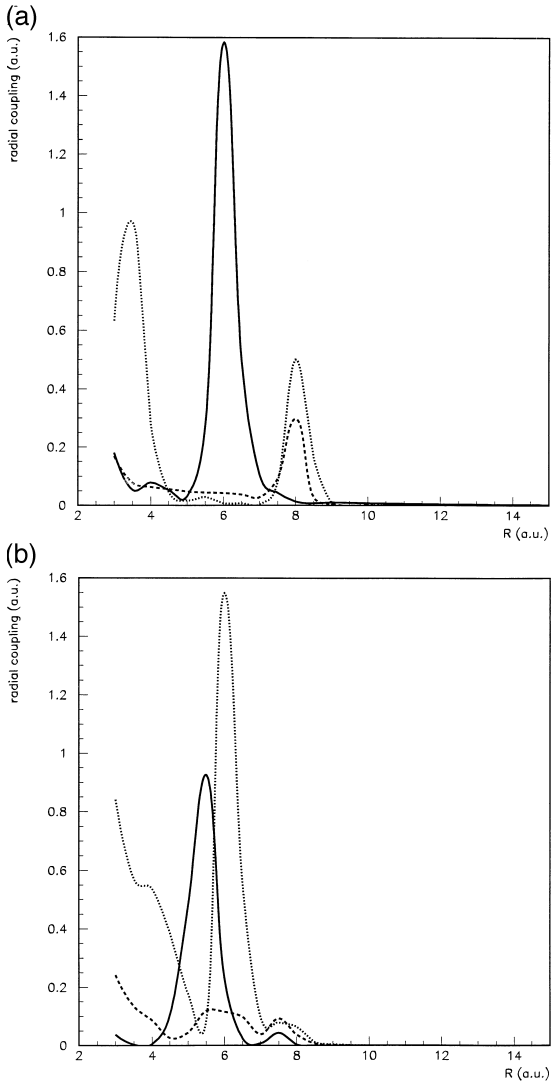

Fig. 2. (a) Non-adiabatic radial coupling matrix elements between $^2\Sigma$ states. — g_{23}; · · · g_{12}; --- g_{13}. (b) Non-adiabatic radial coupling matrix elements between $^2\Pi$ states. — g_{34}; · · · g_{13}; --- g_{14}.

between $^2\Sigma^+$–$^2\Pi$ and $^2\Pi$–$^2\Delta$ molecular states have been determined directly from the quadrupole moment tensor [16].

3. Collision dynamics

Cross sections for capture on the different exit channels have been calculated by a semi classical method using the EIKONXS program [17] for the range of incident ion energies 2–50 keV. The translation effects have been taken into account by introducing common translation factors as proposed by Errea et al. [18].

The partial cross sections for the three main reactions:

$$S^{3+}\left(3s^2 3p\right)^2 P + He\left(1s^2\right)^1 S \rightarrow S^{2+}\left(3s^2 3p^2\right)^1 D + He^+\left(1s\right)^2 S$$

$$S^{3+}\left(3s^2 3p\right)^2 P + He\left(1s^2\right)^1 S \rightarrow S^{2+}\left(3s^2 3p^2\right)^3 P + He^+\left(1s\right)^2 S$$

$$S^{3+}\left(3s^2 3p\right)^2 P + He\left(1s^2\right)^1 S \rightarrow S^{2+}\left(3s^2 3p^2\right)^1 S + He^+\left(1s\right)^2 S$$

corresponding respectively to peaks A, B and C as designed by Wilson et al. [11] have been calculated taking into account the probabilities $1/3$ and $2/3$ for the entry channel to be in a Σ or Π symmetry. The results are displayed in Fig. 3 and Table 2 as well as the ratio of the cross sections σ_B/σ_A which can be directly compared with experimental measurements. An overall good agreement with experimental data is observed for our calculation, in particular the ratio σ_B/σ_A increases with the impact energy and may be

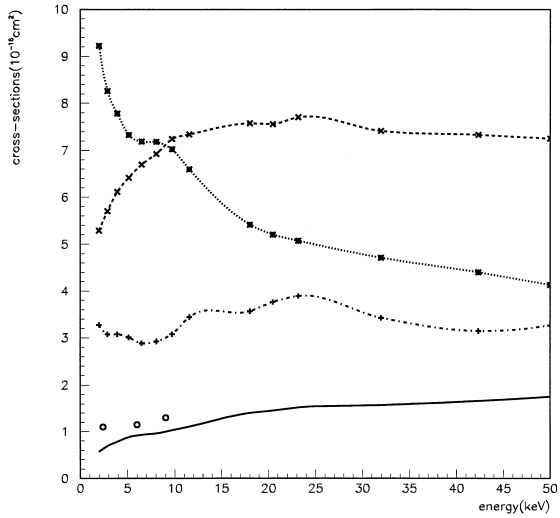

Fig. 3. Partial cross-sections on the $\{S^{2+}(3s^2 3p^2) + He^+\}$ levels with respect to laboratory energies. · · · peak A; --- peak B; · - · peak C; — ratio σ_B/σ_A; ◦ ◦ ◦ experimental ratio ratio σ_B/σ_A (Wilson et al. [11]).

Table 2
Partial and total cross sections for the $S^{3+} + He \rightarrow S^{2+} + He^{+}$ process (in 10^{-16} cm^2).

E_{lab} (keV)	σ_A	σ_B	σ_C	σ_B / σ_A	σ_{tot}
1.98	9.223	5.285	3.271	0.57	17.78
2.89	8.259	5.701	3.078	0.69	17.04
3.92	7.785	6.113	3.076	0.78	16.97
5.12	7.327	6.418	3.009	0.88	16.75
6.49	7.187	6.700	2.883	0.93	16.77
8.02	7.180	6.924	2.925	0.96	17.03
9.69	7.023	7.241	3.079	1.03	17.34
11.53	6.595	7.337	3.443	1.11	17.37
18.02	5.413	7.575	3.567	1.40	16.55
20.45	5.203	7.557	3.765	1.45	16.52
23.15	5.073	7.704	3.893	1.52	16.67
31.98	4.712	7.410	3.427	1.57	15.55
42.34	4.402	7.328	3.147	1.66	14.88
50.00	4.135	7.251	3.270	1.75	14.66

compared quite positively with the experimental spectra. As observed experimentally, the peak A decreases markedly with increasing impact energy although the cross section corresponding to peak B first increases and, from about $E_{lab} = 20$ keV, decreases very slowly. The total cross section remains almost constant all over the collision energy range, about 1.7×10^{-15} cm^2, a value comprised between the values calculated by means of the MCLZ model [11].

4. Concluding remarks

This work provides accurate potential energy curves and coupling matrix elements for the S^{3+}/He system. The results of collision dynamics for the $S^{3+} + He \rightarrow S^{2+} + He^{+}$ reaction are in good agreement with experimental measurements as well as previous MCLZ calculations showing this process as mainly driven by transitions occurring in the neighbourhood of avoided crossings through radial coupling.

References

[1] L. Radom, P.M.W. Gill, M.W. Wong, R.H. Nobes, Pure Appl. Chem. 60 (1988) 183.
[2] D. Péquignot, S.M.V. Aldrovandi, G. Stasinska, Astron. Astrophys. 63 (1978) 313.
[3] S.E. Butler, A. Dalgarno, Astrophys. J. 241 (1980) 838.
[4] R.K. Janev, D.S. Belič, J. Phys. B 15 (1982) 3479.
[5] R.K. Janev, J. Physique 50 (1989) 421, Suppl. no. 1.
[6] M. Gargaud, F. Fraija, M.C. Bacchus-Montabonel, R. McCarroll, J. Phys. B 27 (1994) 3985.
[7] P. Honvault, M. Gargaud, M.C. Bacchus-Montabonel, R. McCarroll, Astron. and Astrophys. 302 (1995) 931.
[8] M.C. Bacchus-Montabonel, Phys. Rev. A 53 (1996) 3667.
[9] M.C. Bacchus-Montabonel, F. Fraija, Phys. Rev. A 49 (1994) 5108.
[10] R. McCray, C. Wright, S. Hatchett, Astrophys. J. 211 (1977) L29.
[11] S.M. Wilson, T.K. McLaughlin, R.W. McCullough, H.B. Gilbody, J. Phys. B 23 (1990) 1315.
[12] B. Huron, J.P. Malrieu, P. Rancurel, J. Chem. Phys. 58 (1973) 5745.
[13] A.D. McLean, G.S. Chandler, J. Chem. Phys. 72 (1980) 5639.
[14] S. Bashkin, J.O. Stoner, Atomic energy levels and Grotrian diagrams, North-Holland, Amsterdam, 1975.
[15] M.C. Bacchus-Montabonel, R. Cimiraglia, M. Persico, J. Phys. B 17 (1984) 1931.
[16] F. Fraija, A.R. Allouche, M.C. Bacchus-Montabonel, Phys. Rev. A 49 (1994) 272.
[17] R.J. Allan, C. Courbin, P. Salas, P. Wahnon, J. Phys. B 23 (1990) L461.
[18] L.F. Errea, L. Mendez, A. Riera, J. Phys. B 15 (1982) 101.